

Group velocity dispersion and self phase modulation in silicon nitride waveguides

D. T. H. Tan,^{a)} K. Ikeda, P. C. Sun, and Y. Fainman

Department of Electrical and Computer Engineering, University of California San Diego,
9500 Gilman Drive, La Jolla, California 92093-0409, USA

(Received 28 October 2009; accepted 4 January 2010; published online 8 February 2010)

The group velocity dispersion (GVD) of silicon nitride waveguides, prepared using plasma enhanced chemical vapor deposition, is studied and characterized experimentally in support of nonlinear optics applications. We show that the dispersion may be engineered by varying the geometry of the waveguide and demonstrate measured anomalous GVD values as high as $-0.57 \text{ ps}^2/\text{m}$ and normal GVD values as high as $0.86 \text{ ps}^2/\text{m}$. We also experimentally demonstrate the absence of any observed nonlinear loss at the telecommunications wavelength at peak intensities of up to $12 \text{ GW}/\text{cm}^2$. Spectral broadening due to self phase modulation in silicon nitride waveguides with a nonlinear parameter of $1.4 \text{ W}^{-1}/\text{m}$ is also demonstrated. © 2010 American Institute of Physics. [doi:10.1063/1.3299008]

In recent years, much work has gone into studying nonlinear phenomena in silicon waveguides. The large nonlinear coefficient and high mode confinement in silicon makes it a good candidate for achieving self phase modulation,¹⁻³ wavelength conversion,^{4,5} and dispersion free propagation in the form of solitons.⁶ In addition, the large refractive index contrast between silicon and its oxide cladding results in a large waveguide contribution to the group velocity dispersion (GVD), enabling a variety of signs and magnitudes of dispersion to be engineered.^{7,8} However, when silicon is used as a nonlinear optical material in the telecommunication frequency range, its relatively small energy band gap causes significant loss from two photon absorption (TPA) and TPA generated free carriers as the mode confinement and input power increases.^{2,3} In contrast, silicon nitride has a larger energy band gap and hence is not expected to have TPA for optical fields in the telecommunication frequency range. It still offers a relatively high refractive index difference with silicon dioxide cladding, supporting dense integration of photonic lightwave circuits (PLCs).^{9,10} In addition, it is compatible with standard complementary metal oxide semiconductor (CMOS) fabrication processes, allowing its integration with the general theme of silicon-based PLCs, designed for fabrication using this mature and cost-effective technology. We recently used plasma enhanced chemical vapor deposition (PECVD) to fabricate silicon nitride, measured its Kerr coefficient, $n_2 = 2.4 \times 10^{-15} \text{ cm}^2/\text{W}$ and fabricated and tested nonlinear optical devices.¹¹ This relatively high measured third order nonlinear coefficient motivated us to continue the study of our silicon nitride material. In this manuscript, we study the dispersive properties of silicon nitride waveguides and show that the GVD can be engineered by changing the waveguide geometry. Moreover, when we increase the input signal power levels of 200 fs pulses derived from an optical parametric oscillator (OPO) operating at a center wavelength of 1550 nm, we observe at the output, spectral broadening due to self phase modulation. We present analyses of these observations, as well as characterize the nonlinear losses in silicon nitride waveguides.

We studied the GVD properties of various silicon nitride waveguide geometries and identified three geometries with representative dispersion properties for demonstration as follows: (i) a 500 nm by $1 \mu\text{m}$ channel waveguide with silicon dioxide cladding, (ii) an 800 nm square channel waveguide with silicon dioxide cladding, and (iii) a $1 \mu\text{m}$ square strip waveguide with air as the upper cladding. Using the Sellmeier coefficients for silicon nitride¹² and silicon dioxide,¹³ the effective indices of the quasi-TE modes in three-dimensions as a function of wavelength are calculated using a fully vectorial beam propagation method from RSOFT. The group indices, n_g and dispersion, β_2 for the waveguides are calculated from the obtained effective indices. The material dispersion of bulk silicon nitride is calculated to be $0.083 \text{ ps}^2/\text{m}$ at a wavelength, $\lambda = 1.55 \mu\text{m}$. Figure 1 shows that we can achieve anomalous dispersion values of $-0.62 \text{ ps}^2/\text{m}$ (strip waveguide) and normal dispersion values as high as $0.58 \text{ ps}^2/\text{m}$ (500 nm by $1 \mu\text{m}$ channel waveguide) at $1.55 \mu\text{m}$. These values are significantly different from the material dispersion of silicon nitride. The effect of the waveguide geometry on the GVD is significant, enabling us to engineer varying magnitudes of either normal or anomalous dispersion. The 500 nm by $1 \mu\text{m}$ channel waveguide and the $1 \mu\text{m}$ strip waveguides result in modes which are more confined, leading to a greater waveguide contribution to the GVD and larger GVD values.

Experimental verification of the GVD is performed using a method similar to that in Ref. 14, where integrated

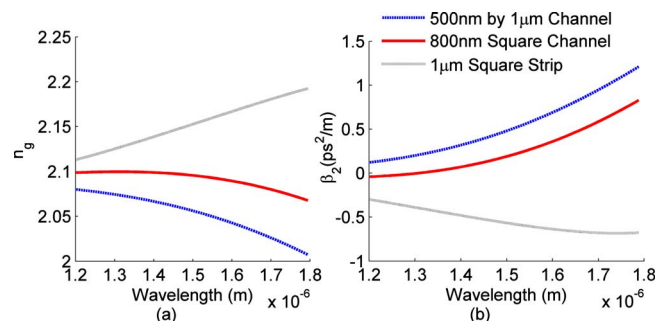


FIG. 1. (Color online) Calculated (a) group index and (b) GVD of silicon nitride waveguides with different geometries.

^{a)}Electronic mail: thtan@ucsd.edu.

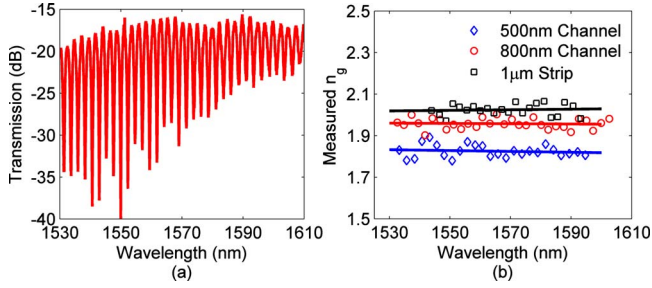


FIG. 2. (Color online) (a) Typical MZI fringes from 800 nm square channel waveguide. (b) Measured group indices for 500 nm by 1 μm channel waveguide (blue diamonds), 800 nm square channel waveguide (red circles) and 1 μm square strip waveguide (black squares).

Mach Zehnder interferometers (MZIs) are fabricated and used to extract the group indices from the resulting oscillations for TE polarized input light. Our waveguide integrated MZIs are fabricated on PECVD prepared silicon nitride films. The deposition process¹¹ results in low stress films and is desirable because of the low process temperature (350 °C). Films between 500 nm and 1 μm in thickness are first deposited. The waveguides are patterned using electron-beam lithography and defined using reactive ion etching.^{9,11} The SiO₂ overcladding of the channel waveguides is deposited using PECVD whereas the strip waveguide is left uncovered. The difference in length between the two arms of the interferometer is 520 μm . To eliminate noise induced error in extracting the GVD, we make a first order approximation to the measured data. Since the expected GVD is approximately constant within the wavelength range of the measurement (1.53–1.6 μm), the average GVD value can be extracted from the gradient of the plot of n_g versus λ using the relation, $\beta_2 = -(\lambda^2/2\pi c^2) \times (dn_g/d\lambda)$. Figure 2(a) shows a typical example of the interference fringes obtained from the MZI implemented with the 800 nm square channel waveguides with SiO₂ cladding. The extracted group indices are shown in Fig. 2(b). The n_g for the 1 μm square strip waveguide is largest followed by the 800 nm square channel waveguide and 500 nm by 1 μm channel waveguide, in agreement with the modeling results shown in Fig. 1. Linear fits to the measured data are applied to each of the plots. Using the extracted value of $dn_g/d\lambda$ for each waveguide, we obtain measured average GVD values of 0.86 ps²/m, 0.28 ps²/m and -0.57 ps²/m for the 500 nm by 1 μm channel, 800 nm square channel and 1 μm square strip waveguides, respectively.

Next, we study the presence of two photon induced optical losses in the silicon nitride waveguides fabricated using PECVD. We use 200 fs pulses centered at 1.55 μm from an OPO pumped by a Ti:Sapphire laser at a center wavelength of 830 nm. A 0.5 nm band pass filter is used to reduce the bandwidth of the ultrashort pulses resulting in ~ 7 ps output pulses. The output from the filter is amplified using an erbium doped fiber amplifier (EDFA) and introduced into a 5 mm long 800 nm square channel waveguide. The output of the waveguide is monitored as we increase the EDFA gain. The long pulse duration ensures negligible temporal pulse broadening in either the fiber or waveguide. Therefore, the peak power may be calculated using the pulse duration, laser repetition rate of 76 MHz and measured average power. We obtain a linear relation between the input and output peak power, shown in Fig. 3(a), implying the absence of nonlinear

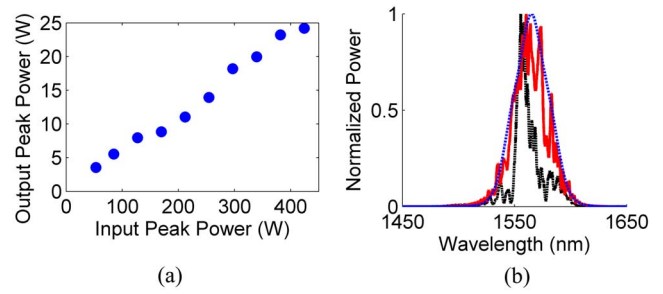


FIG. 3. (Color online) (a) Measured output peak power vs input peak power levels for 800 nm square channel waveguide with silicon dioxide cladding. (b) Spectrum of the measured (solid red line) and modeled (blue dotted line) pulse broadening due to self phase modulation in a 6 mm long silicon nitride channel waveguide (500 nm by 1 μm). In contrast, spectrum measured at low power (black dashed line) does not exhibit waveguide induced spectral broadening.

losses. The experiment confirms that TPA should not occur in silicon nitride at 1.55 μm because photon energies at this wavelength are less than $E_{g(\text{SiN})}/2$, where the energy band gap of silicon nitride, $E_{g(\text{SiN})} = 5.3$ eV. The onset of TPA in silicon nitride is expected at $\lambda \sim 470$ nm in the blue region of the visible spectrum. In contrast, TPA induced loss in silicon is reported to occur at 1.55 μm at peak power intensities > 80 MW/cm² (Ref. 3) for ultrashort pulses and loss from TPA generated free carriers for longer pulses occurs at peak power intensities > 50 MW/cm².² Our waveguide did not exhibit nonlinear losses up to peak power intensities of 12 GW/cm² in the waveguide, which is two orders of magnitude higher than that in silicon. The demonstrated negligible losses at high peak intensities make silicon nitride a better candidate than silicon for nonlinear optics experiments and applications at high power levels.

The different extents of mode confinement in the three waveguides lead to different values of the nonlinear parameter, $\gamma = n_2 \omega_0 / c A_{\text{eff}}$.¹⁵ We obtain a well confined mode with the smallest $A_{\text{eff}} = 0.72$ μm^2 for the 500 nm by 1 μm channel waveguide. Using a previously measured value of $n_2 = 2.4 \times 10^{-15}$ cm²/W,¹¹ we obtain a value of $\gamma_{\text{wg}} = 1.4$ W⁻¹/m for the waveguide. A 500 nm by 1 μm channel waveguide made of silicon nitride with silicon dioxide cladding of length, $L = 6$ mm was fabricated and the measured loss was 4 dB/cm. Next, we demonstrate self phase modulation of 200 fs pulses at 1.55 μm from an OPO. The pulses are first coupled from free space into a fiber before coupling into the silicon nitride waveguide. A single mode tapered fiber is then used to couple the pulses from the OPO into the 6 mm silicon nitride waveguide. Since the high peak power of ultrashort pulses will experience nonlinear effects while propagating in the fiber, we carefully design our experiment to take advantage of the fiber nonlinearity. The interplay between the self phase modulation and anomalous dispersion in the fiber ensures, with careful design of the fiber length, minimal spectral broadening and high peak powers at the output of the fiber. The estimated coupling loss is ~ 7 dB per facet. The experimental results on self phase modulation in the silicon nitride waveguide are shown in Fig. 3(b). First, we measure the output spectrum of the silicon nitride waveguide when the input fiber is deliberately misaligned from the waveguide to ensure low coupled power into the waveguide. The resultant low power spectrum [black dotted curve in Fig. 3(b)] represents a purely linear response

of the pulse propagating in the waveguide, while at the same time exhibiting any nonlinear effects occurring in the preceding fiber used to introduce the pulse into the silicon nitride waveguide. Some Fabry–Perot oscillations are present in the spectrum as a result of the cleaved waveguide facets and stitching error in the 6 mm long waveguide. Next we optimize the alignment of the fiber to waveguide setup to achieve maximum coupling into the silicon nitride waveguide. We estimate $P_o \sim 500$ W inside the waveguide by including the coupling loss and estimated peak power at the entrance to the waveguide. The red solid line in Fig. 3(b) shows the spectrum of the pulse at the output of the waveguide demonstrating appreciable spectral broadening. Comparing the full width at half maximum (FWHM) of the broadened (red solid line) and the original spectra (black dashed line), the bandwidth has doubled from 14 to 30 nm. The broadening is attributed to self phase modulation of the pulse in the silicon nitride waveguide, which occurs due to the Kerr nonlinearity.¹¹

Modeling of our experiments using the nonlinear Schrödinger equation (NLSE) (Ref. 15) was performed to confirm the measured experimental results. The effect of self phase modulation arising from the optical nonlinearity in the silicon nitride waveguide was modeled using the measured value of $\beta_{2\text{wg}}=0.86$ ps²/m, the calculated value of $\gamma_{\text{wg}}=1.4$ W⁻¹/m and the experimentally measured loss coefficient, $\alpha_{\text{wg}}=0.92$ /cm. The third order dispersion length for the waveguide is calculated to be $\gg L$ and therefore may be neglected. The input used in the model is a fit to the measured fiber output spectrum shown in Fig. 3(b). The blue dotted curve in Fig. 3(b) shows the solution to the NLSE for the spectrum broadened by the waveguide. The estimated maximum nonlinear phase shift from the waveguide is about π radians. The extent of self phase modulation in the waveguide is limited by the propagation loss in the waveguide. Propagation loss is related to the waveguide effective length, $L_{\text{eff}}=[1-\exp(-\alpha_{\text{wg}}L)]/\alpha_{\text{wg}}$.¹⁵ For the PECVD waveguides used in our experiment with 4 dB/cm loss, the maximum achievable effective length, $L_{\text{eff(max)}}$ asymptotically approaches a value of $1/\alpha_{\text{wg}}=1.1$ cm. Calculations show that reducing the loss to 1 dB/cm will enable about 30% greater broadening, for the same waveguide length and conditions used in the experiment. In addition, reduction of the loss will allow a larger $L_{\text{eff(max)}}$ to be achieved, and hence enable even greater spectral broadening by increasing the waveguide length. Lower propagation losses may be achieved by high temperature annealing¹⁶ to reduce the hydrogen content in the films and loss from material absorption or using films prepared using low pressure chemical vapor deposition.^{10,17,18}

We have shown that silicon nitride waveguides fabricated from PECVD deposited films are viable nonlinear materials for various devices integrated into PLC. The low temperature deposition process is economical and compatible

with CMOS fabrication processes. The GVD of several silicon nitride waveguides has been studied experimentally in support of nonlinear optical interactions in this material. The results show that the GVD may be engineered by varying the geometry of the waveguide and demonstrate measured anomalous GVD values as high as -0.57 ps²/m and normal GVD values as high as 0.86 ps²/m. The absence of any observed nonlinear loss implies that high power levels may be used in silicon nitride waveguides for nonlinear optics applications without degradation due to TPA processes common to silicon at the telecommunications wavelength. Self phase modulation occurring in the fabricated silicon nitride waveguides is also experimentally demonstrated. A doubling of the FWHM pulse bandwidth is observed as a result of the nonlinear parameter of 1.4 W⁻¹/m in the silicon nitride waveguide. The relatively high nonlinear parameter, low nonlinear loss and ability to engineer GVD in waveguides make silicon nitride a good candidate for realizing a variety of optical functionalities utilizing nonlinear optical phenomena such as four wave mixing,¹⁸ soliton propagation, and pulse compression.

This work was supported by the Defense Advanced Research Projects Agency, the National Science Foundation, the NSF CIAN ERC, and the U.S. Army Research Office.

¹O. Boyraz, T. Indukuri, and B. Jalali, *Opt. Express* **12**, 829 (2004).

²E. Dulkeith, Y. A. Vlasov, X. Chen, N. C. Panoiu, and R. M. Osgood, Jr., *Opt. Express* **14**, 5524 (2006).

³I.-W. Hsieh, X. Chen, J. I. Dadap, N. C. Panoiu, R. M. Osgood, S. J. McNab, and Y. A. Vlasov, *Opt. Express* **14**, 12380 (2006).

⁴H. Fukuda, K. Yamada, T. Shoji, M. Takahashi, T. Tsuchizawa, T. Watanabe, J.-i. Takahashi, and S.-i. Itabashi, *Opt. Express* **13**, 4629 (2005).

⁵M. A. Foster, A. C. Turner, J. E. Sharping, B. S. Schmidt, M. Lipson, and A. L. Gaeta, *Nature (London)* **441**, 960 (2006).

⁶J. Zhang, Q. Lin, G. Piredda, R. W. Boyd, G. P. Agrawal, and P. M. Fauchet, *Opt. Express* **15**, 7682 (2007).

⁷A. C. Turner, C. Manolatu, B. S. Schmidt, M. Lipson, M. A. Foster, J. E. Sharping, and A. L. Gaeta, *Opt. Express* **14**, 4357 (2006).

⁸D. T. H. Tan, K. Ikeda, and Y. Fainman, *Appl. Phys. Lett.* **95**, 141109 (2009).

⁹T. Barwicz, M. A. Popovic, M. R. Watts, P. T. Rakich, E. P. Ippen and H. I. Smith, *J. Lightwave Technol.* **24**, 2207 (2006).

¹⁰W. Stutius and W. Streifer, *Appl. Opt.* **16**, 3218 (1977).

¹¹K. Ikeda, R. E. Saperstein, N. Alic, and Y. Fainman, *Opt. Express* **16**, 12987 (2008).

¹²A. M. Pérez, C. Santiago, F. Renero, and C. Zuniga, *Opt. Eng.* **45**, 123802 (2006).

¹³G. P. Agrawal, *Lightwave Technology: Components and Devices* (Wiley, Hoboken, NJ, 2004).

¹⁴E. Dulkeith, F. Xia, L. Schares, W. M. Green, L. Sekaric, and Y. A. Vlasov, *Opt. Express* **14**, 6372 (2006).

¹⁵G. P. Agrawal, *Nonlinear Fiber Optics* (Academic, Boston, MA, 1995).

¹⁶C. Boehme and G. Lucovsky, *J. Vac. Sci. Technol. A* **19**, 2622 (2001).

¹⁷A. Gondarenko, J. S. Levy, and M. Lipson, *Opt. Express* **17**, 11366 (2009).

¹⁸J. S. Levy, A. Gondarenko, M. A. Foster, A. C. Turner-Foster, A. L. Gaeta, and M. Lipson, *Nat. Photonics* **4**, 37 (2009).